A Case of Childhood Tuberculosis from Late Mediaeval Somerset, England.

Dawson-Hobbis H[1], Taylor GM[2*], Stewart GR[2].

1. Department of Archaeology, Anthropology and Geography, Sparkford Road, University of Winchester, Winchester, Hampshire, SO22 4NW, UK.

2. Department of Microbial and Cellular Sciences, Faculty of Health and Medical Sciences, University of Surrey, Guildford, Surrey, GU2 7XH, UK.

*Corresponding author:

Prof. G. Michael Taylor,

Department of Microbial and Cellular Sciences,

Faculty of Health and Medical Sciences,

University of Surrey, Guildford,

Surrey, GU2 7XH, UK.

Gm.taylor@surrey.ac.uk.

This is an accepted manuscript of an article published by Elsevier in Tuberculosis, available online at https://doi.org/10.1016/j.tube.2021.102088. It is not the copy of record. Copyright © 2021, Elsevier.

Manuscript File

Click here to view linked References

A Case of Childhood Tuberculosis from Late Mediaeval Somerset, England.

Dawson-Hobbis H[1], Taylor GM[2*], Stewart GR[2].

1. Department of Archaeology, Anthropology and Geography, Sparkford Road, University of Winchester, Winchester, Hampshire, SO22 4NW, UK.

2. Department of Microbial and Cellular Sciences, Faculty of Health and Medical Sciences, University of Surrey, Guildford, Surrey, GU2 7XH, UK.

*Corresponding author:

Prof. G. Michael Taylor,

Department of Microbial and Cellular Sciences,

Faculty of Health and Medical Sciences,

University of Surrey, Guildford,

Surrey, GU2 7XH, UK.

Gm.taylor@surrey.ac.uk.

This is an accepted manuscript of an article published by Elsevier in Tuberculosis, available online at https://doi.org/10.1016/j.tube.2021.102088. It is not the copy of record. Copyright © 2021, Elsevier.

ABSTRACT.

Background.

The remains of a 3-5 year-old child from the late medieval cemetery serving the Priory of St. Peter and St. Paul, Taunton, Somerset, UK was the subject of an aDNA study.

Objective.

The aim was to distinguish between two differential diagnoses suggested by earlier osteological examination of the remains; either tuberculosis or Langerhans cell histiocytosis.

Findings.

The remains tested positive for MTB complex markers, corroborating this diagnosis reached on osteological grounds. Based on positivity for the *mtp40* element and a deletion in the *pks15/1* locus, we conclude that infection was due to a strain of the human pathogen *M.tuberculosis* belonging to lineage 4 . Although DNA recovered from the case was heavily fragmented, sex determination by amelogenin PCR suggested these are the remains of a young male child. The findings are discussed considering additions to the literature since the original report.

Conclusions.

Descriptions of tuberculosis in children from this period are rare and burial SK2077 represents the first UK example of a pre-adolescent individual to have a molecular diagnosis combined with osteological pathology. This provides an important reference of childhood tuberculosis and insight into the likely presence of tuberculosis in the mediaeval adult population served by this cemetery.

Keywords. Tuberculosis, extrapulmonary, mediaeval, Taunton, *mtp40* PCR.

This is an accepted manuscript of an article published by Elsevier in Tuberculosis, available online at https://doi.org/10.1016/j.tube.2021.102088. It is not the copy of record. Copyright © 2021, Elsevier.

1.1 BACKGROUND.

One of us (HD-H) has previously described the remains of a young child (AD 1150-1539) from the late mediaeval cemetery associated with the Priory of St. Peter and St. Paul, Taunton, Somerset, UK [1]. The priory was an Augustinian house of canons founded in the early 12th century by William Giffard (or Gyffarde), Lord Chancellor of England (1093-1101) and Bishop of Winchester (1100-1129 AD). The Priory was in use until the Dissolution in 1539 AD and much of it was demolished by the mid 16th century [2]. Osteological analysis carried out on 190 inhumations excavated during 2005 showed a mixed cemetery population, indicating it served a lay community [3].

The remains under review in the present study, Sk2077, come from burials recovered from area 4 of the 2005 excavations, sited towards what appears to be the northern edge of the cemetery (Figure 1).

The remains are those of a young child aged between 3-5 years at the time of death. A number of skeletal indicators suggested a probable diagnosis of tuberculosis. These included a circular lytic lesion on the right parietal bone at the posterior medial corner, close to where the sagittal and lambdoidal sutures meet. The cranial lesion penetrates through both the inner and outer tables as a circular hole 10mm in diameter. Ectocranially, the hole has a smooth edge and some porosity surrounds the area. The endocranial surface has a larger circular area of bone destruction, involving the diploic space, 16mm in diameter with a sharp edge. The occipital bone exhibits resorptive endocranial lesions, also known as *serpens endocrania symmetrica* (SES) along the area of the occipital sulcus, covering 45mm length and 12-15mm width. There are slight lytic lesions on the atlas, on the superior edge of the posterior rim, and on the axis, on the inferior edge of the lamina; destructive lytic lesions on the visceral surface of three rib fragments and a small area of periostitis (woven bone) present on one rib and periosteal new bone formation (woven bone) on both femora [1]. It has been shown that in documented cases of tuberculosis in juveniles, periosteal reaction on long bones may not be uncommon [4]. An alternative diagnosis considered at the time of the previous examination was eosinophilic granuloma, a variant of Langerhans cell histiocytosis [5]. The main aim of the present study was to investigate and if possible confirm the diagnosis of tuberculosis using an ancient DNA (aDNA) approach.

This is an accepted manuscript of an article published by Elsevier in Tuberculosis, available online at https://doi.org/10.1016/j.tube.2021.102088. It is not the copy of record. Copyright © 2021, Elsevier.

2. METHODS.

2.1 Estimation of age.

SK2077 was aged by dental eruption and formation [6]; radiographs of the sub-adult mandibles from this collection were taken, where intact, to aid in the identification of tooth formation stages; this was the case for SK2077.

2.2 Samples collected.

Bone samples were collected from three locations on the skeleton of individual Sk2077 for aDNA analysis. These sites included fragments of two ribs, one with a lytic lesion and a section of the posterior rim of the atlas with lesion. Initially, DNA extracts were prepared from bone powder taken from the two ribs. These ranged from 80 to 152 mg. The cervical vertebra (atlas) was treated differently to avoid any destruction of the sample and lesion. It was immersed in 5ml of 6M GUSCN extraction buffer in a 50ml conical tube and gently vortex-mixed several times over the course of 1hr. It was then left for one week at 37^0C to prevent buffer precipitation. Buffer was recovered by gentle centrifugation (2000 x rpm for 10 mins) and taken forward for DNA recovery using a silica slurry (see below). The atlas sample was washed in an ascending alcohol series (50, 70 and 100% ethanol) to remove residual GUSCN traces and then air-dried. It was eventually returned to the other elements of the burial.

2.3 DNA extraction.

The bone samples were taken through a GUSCN/silica DNA extraction procedure [7], a modification of the original Boom method [8]. DNA was eluted from the silica in either 65µl (ribs) or 30µl (atlas) of HPLC grade water.

2.4. PCR methods.

2.4.1. Mycobacterium tuberculosis (MTB) complex species.

A PCR for the IS*6110* insertion element was performed as previously described [9]. This is a modification of the method originally reported by Thierry and colleagues (1990) [10]. The element can be present from low to high copy number in isolates of *M.tuberculosis*. Copy number and preferential insertion site of IS*6110* are linked to tuberculosis lineages, reflecting ancestral phylogeography [11]. Whilst some isolates from Southeast Asia can lack IS*6110* [12] these are

This is an accepted manuscript of an article published by Elsevier in Tuberculosis, available online at https://doi.org/10.1016/j.tube.2021.102088. It is not the copy of record. Copyright © 2021, Elsevier.

extremely unlikely to be encountered in European strains. Extracts were also tested with a second PCR for the IS element IS*1081*, which is present in 6 copies in members of the MTB complex. A variety of IS*1081* primer combinations were used to assess template size preservation in the extracts [13,14]. A dual-labeled hybridization probe [(HEX) 5'-ATT GGA CCG CTC ATC GCT GCG TTC GC-3' (BHQ-1)] was used to report formation of any product.

2.4.2. Differentiation of *M.tuberculosis* complex species.

A polymerase chain reaction (PCR) for *mtp40* was performed using primers which amplify a 113-bp fragment from the *mpcA* gene (Rv2351c). The sequences of these were: F 5'-GGTCTGGTCGAATTCGGTGGAGT-3 and R 5'-ATTCGCGCCCGGTTCGGCGT-3'. The *mtp40* element can be used to identify differences within the *M. tuberculosis* complex. It is present in the vast majority of *M. tuberculosis* isolates and absent from *M. bovis* isolates. It was originally thought that some strains of *M.bovis* retained *mtp40* [15,16] but these have since been shown to be strains of *M.africanum* [17], which are endemic in West Africa and unlikely to have been present in mediaeval Somerset. Absence of *mtp40* from *M. bovis* strains is associated with RD5, an early deletion event in the evolution of the MTB complex. RD5 is 8,964 nucleotides in size and located between genome positions 2,626,067–2,635,031 on the H37Rv reference strain [18].

2.4.3. Genotyping using the polymorphic pks15/1 locus of *M.tuberculosis* complex.

We amplified the pks15/1 polymorphic locus to determine whether a characteristic 7-bp deletion event had occurred in the Sk2077 isolate [19]. The forward and reverse primers used were: F 5'-GCCATAAGTCGACCCGCCTGC-3' and 5'-GCAGAGGCGCCGGTTGAGGC-3'. These generate a 118-bp amplicon from strains belonging to lineage 4 (L4 or Euro-American) and 125-bp from other *M.tuberculosis* lineages. Amplicon formation was monitored using a specific dual-labelled hydrolysis probe (5'[HEX]AAAGCACCGGGGGCCGCGGCCGTCGAT[BHQ1]-3'). The products were run out on 3% agarose gel to check size and excised bands were purified using a Geneclean DNA isolation kit (Cat. No.1001– 200, MP Biomedicals, California, USA). These were Sanger sequenced at Genewiz Ltd., Takely, Essex, UK.

2.4.4. Screening for brucella species DNA.

Brucellosis is often a differential diagnosis in skeletal tuberculosis involving the spine and weight-bearing joints [20]. Therefore the extract prepared from the rib with a lytic lesion was tested for

This is an accepted manuscript of an article published by Elsevier in Tuberculosis, available online at https://doi.org/10.1016/j.tube.2021.102088. It is not the copy of record. Copyright © 2021, Elsevier.

brucella pathogen DNA by PCR with primers which amplify an 85-bp fragment from the IS*711* repetitive element. This is conserved in multiple copies across the brucella species and biovars. Product was reported using a specific FAM/BHQ1 dual-labelled hybridization probe (Table S3, Supporting information in Bendrey et al, 2020) [21].

2.5. Sex determination by amelogenin PCR.

A sex-determining PCR based on polymorphisms in the amelogenin gene was also applied. In this method, males are identified by two PCR bands, one of 105-bp from the Y chromosome and another of 290-bp from the X chromosome. Females generate only the 290-bp product. The sequences of the primers used in this method were (F2) 5'-TGACCAGCTTGGTTCTAWCCC- 3' and reverse (R1) 5'-CARATGAGRAAACCAGGGTTCCA-3' [22].

2.6. PCR reaction conditions.

PCR for all methods was performed in a final volume of 15 µl, using the HotStart Taq Master Mix Kit from Qiagen (product 203445). The reactions contained 25 pmol of forward and reverse primers, each in 1 µl, 7.5 µl of kit master mix, 1.5-µl non-acetylated bovine serum albumin (BSA, 10 mg ml^{-1}, Sigma B4287) and 3 µl of the template. The intercalating dye EVAGreen® (Biotium, code BT31000) was used to report product formation in non probe-based PCR reactions. The kit magnesium ion concentration of 1.5mM per reaction was supplemented to 2mM for PCR methods using EVAGreen® dye and to 3mM $MgCl_2$ for real-time PCR when using any of the labeled hybridization probes. All probes were used at a final concentration of 100 nM. The volumes were made up to 15 µl with molecular biology grade water (Sigma-Aldrich). After an initial activation step of 14 min at 95^0 C, 41-45 cycles of amplification were performed on an Mx3005P RT-PCR platform (Agilent Technologies). When using the GC-rich pks15/1 probe, an extra 4^{th} PCR step of 10s was included to acquire fluorescence data at 85C. Non-template controls contained water in place of DNA extract.

2.7. Gel electrophoresis.

PCR products were run out on 3% agarose gels in a TAE buffer system alongside DNA size markers (100-bp DNA ladder, Promega) to confirm amplicon size.

2.8. Measures to prevent contamination.

This is an accepted manuscript of an article published by Elsevier in Tuberculosis, available online at https://doi.org/10.1016/j.tube.2021.102088. It is not the copy of record. Copyright © 2021, Elsevier.

188 Separate laboratories were used for each of the three main stages of the aDNA analyses, these
189 being extraction, amplification and post-PCR steps such as gel electrophoresis. The pre- and post-
190 PCR laboratories were physically separated and independently equipped with pipettes, fridge
191 freezers, mixers and bench top centrifuges, disposable plastic ware, filter pipette tips and other
192 reagents dedicated to the project. Surfaces and equipment in the clean 'set-up' laboratory in
193 contact with sample tubes (centrifuges, rotors, mixers, etc.) were cleaned before each assay.
194 Template blanks were run alongside bone extracts in the PCR machine to screen for random
195 contamination. Except for one amelogenin PCR, positive controls were not included in any of the
196 experiments.
197

This is an accepted manuscript of an article published by Elsevier in Tuberculosis, available online at https://doi.org/10.1016/j.tube.2021.102088. It is not the copy of record. Copyright © 2021, Elsevier.

198 ## 3. RESULTS.

199 ### 3.1. Estimation of age.

200 Based upon formation and eruption of the dentition, age of individual Sk2077 was estimated to be
201 3-5 years of age at the time of death.
202

203 ### 3.2. MTB complex screening.

204 a). Both rib extracts and the atlas were all found to be positive for IS*6110* PCR. This IS element can
205 be present in up to 30+ copies in the *M. tuberculosis* genome, depending on strain lineage and is
206 one of the most sensitive markers of complex members. Figure 2 shows IS*6110* amplification and
207 dissociation profiles (melt analysis) in the extracts from one of the rib samples and from the atlas.
208

209 The extract prepared from the atlas displayed a shallower amplification profile, reaching a lower
210 final fluorescence value compared to the rib extract. This was also reflected in the melt analysis
211 curve. This might suggest that inhibitors of the PCR reaction could have been co-extracted along
212 with remnant aDNA templates. A number of substances present in the environment are known to
213 cause PCR inhibition, particularly humic and fulvic acids [23, 24] and can quench fluorescence
214 values. In most instances, the amplification buffer system we use, which includes a final
215 concentration of 1mg/ml non-acetylated BSA, overcomes such problems.
216

217 b). Screening for the IS element IS*1081* was successful when applied to the extract prepared from
218 the atlas (Figure 3). However, we found that successful product amplification size was restricted to
219 primers which generated an amplicon of 79-bp and was not positive when trying to amplify either
220 135-bp templates or the intermediate size of 113-bp, suggesting particularly fragmented DNA
221 (Table 1).
222

223 ### 3.3. Species testing with *mtp40* PCR.

224 The extract prepared from the atlas was tested for the *mtp40* element and was found to be
225 positive (Figure 4). Repeat testing for IS*6110* was performed at the same time and this test was
226 again seen to be positive, generating the expected 123-bp product.
227

228 ### 3.4. Genotyping using the polymorphic pks15/1 locus.

This is an accepted manuscript of an article published by Elsevier in Tuberculosis, available online at https://doi.org/10.1016/j.tube.2021.102088. It is not the copy of record. Copyright © 2021, Elsevier.

The real-time PCR probe for the pks15/1 locus reported product formation in duplicate samples of the atlas extract (Figure 5a). Subsequent gel electrophoresis showed band sizes of about 120-bp. When sequenced, the amplicon clearly showed that it was identical to lineage 4 isolates of the *M.tuberculosis* complex in which a 7-bp deletion event has occurred (Figure 5b).

3.5. Screening for brucella species DNA.

There was no indication of brucella pathogen DNA in either of the ribs or cervical vertebra.

3.6. Sex determination by amelogenin PCR.

One of the two rib extracts generated a single peak on real-time PCR which melted at 79.7^{0}C, the same temperature as the Y chromosome product in the melt curve analysis (Figure 6, panel a). Furthermore, when run out on a 3% agarose gel the product was seen to be a single band of expected size (Ca. 105-bp), matching the male reference sample smaller band (Figure 6, panel b). The second expected X chromosome product of 290-bp was not amplified from Sk2077, consistent with heavily fragmented template DNA in this individual.

This is an accepted manuscript of an article published by Elsevier in Tuberculosis, available online at https://doi.org/10.1016/j.tube.2021.102088. It is not the copy of record. Copyright © 2021, Elsevier.

4. DISCUSSION.

A re-examination of the remains of Sk2077 has confirmed a diagnosis of infection with a member of the MTB complex. This is indicated by the positive PCR findings for both IS*6110* and IS*1081*. The fact that Sk2077 was additionally positive for the *mtp40* element indicates that the species involved was a strain of *M.tuberculosis sensu stricto*, rather than *M.bovis* as the latter have lost this locus as part of the RD5 deletion event [18]. Further genotyping with the polymorphic pks15/1 locus showed that a 7-bp deletion, characteristic of lineage 4 had occurred. Strains of *M.tuberculosis* with this deletion are deficient in the production of phenolphthiocerol derivatives [19]. The isolate in Sk2077 therefore belongs to this ancestry, sometimes referred to as the Euro-American lineage [25]. This is one of the more globally widespread of the *M.tuberculosis* lineages.

All the biomolecular findings indicated that DNA remaining in the burial was heavily fragmented. For this reason and to avoid further destruction of precious material, Individual Sk2077 was not considered to be a suitable candidate for wider genome characterisation by next generation sequencing (NGS). A non-destructive means of DNA extraction was tried here for the atlas bone and this allowed a fairly easy means of preserving an important specimen without loss of the physical lesions. The GUSCN buffer and vortex mixing dislodged some looser bone particles but otherwise the sample showed no evidence of having been processed and was eventually returned to the burial.

Although unlikely, our study does not completely rule out that the individual may have suffered from concomitant Langerhans cell histiocytosis (LCH). The etiology of LCH is still poorly understood but there is growing evidence to suggest that it represents a rare cancer and is associated with specific gene mutations. The most frequent genetic association is with the oncogenic V600E BRAF mutation, which has been reported to occur in approximately 60% of LCH cases [26]. Assay of aDNA for such markers of LCH, and indeed other non-communicable diseases, is possible but due to the limited and degraded DNA, we restricted our “host” analysis in this study to sex determination.

Thus, as well as demonstrating the presence of tuberculosis pathogen DNA, we were able to show that the remains were those of a young male child. In adults the overall tuberculosis sex ratio

This is an accepted manuscript of an article published by Elsevier in Tuberculosis, available online at https://doi.org/10.1016/j.tube.2021.102088. It is not the copy of record. Copyright © 2021, Elsevier.

(male: female) is often quoted at around 2:1 [27,28]. However, the male: female ratio of tuberculosis infection for younger children like Sk2077 is nearer 1:1. This ratio increases with age, with males having a higher ratio than females from the 2nd decade onwards, peaking in the 6th decade (to 3.4:1) then decreasing until the eighth decade, when it rises again [28]. However, Information for the male: female ratio of tuberculosis in the medieval period is lacking.

In children of this age (3-5 years), infection is often the result of exposure to an infected adult, usually a parent or other household member with contagious pulmonary tuberculosis. The positivity of Sk2077 infers that it is very likely that tuberculosis was present amongst the adult population that this cemetery served, even though it may not be apparent on the skeletal remains. This is unsurprising, as only a small percentage of tuberculosis cases result in characteristic skeletal patterning [29].

Young children once exposed, also have a higher risk of progression to disease and are more likely to develop severe or disseminated TB. It is thought that up to 50% of children exposed to tuberculosis may go on to develop symptoms of the disease within 6-9 months. In comparison, the rates in immuno-competent adults exposed to tuberculosis may be only 5-10% over the course of their whole lifetime [30].

The bone lesions indicative of tuberculosis in Sk2077 point to a chronic infectious process of at least several months duration or possibly longer [31]. The rib lesions and other widespread signs of tuberculosis suggest this probably started in the lungs and spread to the ribs, lymph nodes [32] and other soft tissues, followed by other parts of the skeleton including the cranium, possibly ultimately resulting in tuberculous meningitis. Calvarial involvement is generally a very rare manifestation of extrapulmonary tuberculosis. The spread to the right parietal bone in Sk2077 may have been via the haematogenous route with seeding to the spongy cancellous diploë separating the inner and outer layers of skull cortical bone [33].

Since Dawson and Robson Brown (2012) [1] published their initial findings on Sk2077, research into the palaeopathology of children has continued to flourish with new comparison studies illustrating the presence of the types of lesions present on Sk2077 and their association with TB as cause of death.

Clinical cases of cranial lesions in association with TB in living individuals have been reported by

This is an accepted manuscript of an article published by Elsevier in Tuberculosis, available online at https://doi.org/10.1016/j.tube.2021.102088. It is not the copy of record. Copyright © 2021, Elsevier.

Datta *et al*. 2017 [34], including a young adult male exhibiting a 4-mm defect in the outer table of the calvaria near the parieto-occipital suture and an adolescent girl with lytic destruction of the left frontal and squamous part of the temporal bone. Archaeological examples with lesions similar to those on Sk2077 are presented in Table 2.

Lytic cranial lesions have been reported by Columbo *et al*. (2015) [35] on a mediaeval child (1-2.5 years) from France, and they also suggested a diagnosis of either Langerhans cell histiocytosis or TB, or in fact perhaps both conditions, as well as by Abegg *et al*. (2020) [36] on a Neolithic child (2-6 years) from Switzerland, and Geber (2015) [37] on a post medieval child (9 years) from Ireland. Examples of endocranial lesions (SES) in association with periosteal new bone formation (PNB) on the long bones have been reported by Hershkovitz *et al*. (2015) [38], Abegg *et al*. (2020) [36] and Collins (2020) [39]. Hershkovitz *et al*. (2015) [38] detected *M. tuberculosis* aDNA from an infant Neolithic skeleton from Atlit-Yam in the Eastern Mediterranean. The infant had both endocranial lesions (*SES*) and periosteal lesions on the long bones, whilst a young adult female in the same grave presented periosteal lesions on one tibia bone also tested positive.
Lytic lesions on the ribs of a 9-10 year old child from a Christian cemetery site, Roman Pécs, Hungary, show a similar scooped out appearance to those of Sk2077 and were reported in association with more classic lesions of the vertebrae causing collapse and kyphosis [40]; periosteal new bone formation was also noted on the femur and tibia. Molecular analysis was undertaken in this case but the sequencing failed to provide sufficient data for a diagnosis.

The presence of lesions on the cervical vertebrae, as seen in Sk2077, appears to be rare in the literature, something noted by Lewis in 2018 [41]. Spekker *et al*. [42] present a case of TB from a 12 year old child with pitting and slight cortical remodelling on the first to fifth cervical vertebrae with more marked destructive lesions on the rest of the spine. Pitting was also noted on the proximal ends of the ribs. A case of a five year old child from Neolithic Italy has clustered pitting and cavitation on the inferior surface of the body of the fourth cervical vertebra alongside evidence for lytic lesions on the ribs and some PNB on the long bones (Sparacello *et al*. 2017) [43]. Cases described by Walker (2012) [44] and Collins (2020) [39] show lytic activity affecting the laminae of the atlas and/or cervical vertebrae (as was seen in the atlas and axis of Sk2077) a diagnosis of possible TB was given in these cases. One case of a 17 year-old male from the Terry Anatomical collection, USA and known to have died from TB in the twentieth century, shows destructive lesions of the atlas [45], although in this case most of the vertebral column was also

This is an accepted manuscript of an article published by Elsevier in Tuberculosis, available online at https://doi.org/10.1016/j.tube.2021.102088. It is not the copy of record. Copyright © 2021, Elsevier.

affected by destructive lesions.

Relatively little is known of TB lineages present in archaeological material from Britain. The earliest confirmed case of tuberculosis in Britain dates to the late Iron Age and comes from Tarrant Hinton in Dorset [46]. It involved a male individual of about 40 years of age at death showing signs of Pott's disease. Genotyping showed this was due to a strain of *M.tuberculosis* rather than *M.bovis*. In addition, the strain was shown to have undergone the TbD1 deletion, indicating the isolate would belong to one of three possible lineages of "modern" *M.tuberculosis*, these being lineages two, three or four [25].

In a wide-ranging study of British and European cases of probable TB Müller et al, (2014) [47] confirmed the pathogen DNA in a total of eight cases from Britain using PCRs for both IS*6110* and IS*1081* insertion elements, with confirmation by either probe or sequencing of the cloned amplicons. The dates of these cases ranged from 11th to mid 19th centuries. They confirmed that ribs with visceral lesions were generally good samples to select to study for evidence of MTB complex DNA. However, there was no attempt to identify the species involved or to which lineages the strains belonged.

A study of burials from the deserted mediaeval village of Wharram Percy (WP) verified ancient TB DNA in a total of nine cases. Six were male and three female, with ages ranging from 25-50 plus years. The dates of these individuals spanned from early 10th right up to late 16th century [48]. A variety of genotyping PCRs were applied and all cases were again found to be due to *M.tuberculosis sensu stricto* based on either a characteristic mutation in the o*xyR* pseudogene, or the presence of species-specific spacer patterns in the spoligotyping procedure [49].

A further three cases of tuberculosis including burials G658, EE002, and EE005 (all juveniles, with age estimated around 10-11 years) from WP were later identified through the study of individuals either with or without periostitic rib lesions, seen as a proxy marker for pulmonary tuberculosis [50]. One further individual from WP, EE062, a male aged 30-40 years with hypertrophic pulmonary osteopathy (HPO) was also found to be positive for a strain of *M.tuberculosis* [51], suggesting HPO was induced by tuberculosis infection in this case.

Finally, Bouwman and colleagues [52] used hybridization sequence capture followed by next

This is an accepted manuscript of an article published by Elsevier in Tuberculosis, available online at https://doi.org/10.1016/j.tube.2021.102088. It is not the copy of record. Copyright © 2021, Elsevier.

generation sequencing (NGS) to successfully analyse a strain of *M.tuberculosis* recovered from a 19th century female burial (Sk4006, 16-18 years) from St. George's crypt, Leeds, West Yorkshire. Additionally, a number of loci were independently amplified by PCR and sequenced to confirm the capture array data. The strain found by these workers can also be described as "modern", having lost the TbD1 deletion. It had also undergone the 7-bp deletion in the *pks15/1* locus, indicating it too belonged to the Euro-American clade (lineage 4). This remains one of the most fully typed historic isolates of *M.tuberculosis* from Britain, although late in the sequence of known cases.

This is an accepted manuscript of an article published by Elsevier in Tuberculosis, available online at https://doi.org/10.1016/j.tube.2021.102088. It is not the copy of record. Copyright © 2021, Elsevier.

5. CONCLUSIONS.

Biomolecular analysis extracts prepared from skeletal elements of a young child from late mediaeval Taunton, Somerset, England confirmed a diagnosis of infection with a strain of *M.tuberculosis* belonging to lineage 4. These findings point to the presence of tuberculosis in adult members of the same mediaeval community. Sex determination using amelogenin PCR was able to show these were the remains of a young male child.

This is an accepted manuscript of an article published by Elsevier in Tuberculosis, available online at https://doi.org/10.1016/j.tube.2021.102088. It is not the copy of record. Copyright © 2021, Elsevier.

ACKNOWLEDGEMENTS.

We thank Professor Katherine Robson Brown, Director of the Jean Golding Institute, University of Bristol, UK for providing access to material from the Taunton cemetery site and Mr. Richard McConnell and Dr. Cheryl Green of Context One Archaeological Services, Dorset, UK for access to the images from the excavation archive. Last, but not least, we are grateful to the two anonymous referees for the time spent in reviewing our manuscript and their constructive comments.

This is an accepted manuscript of an article published by Elsevier in Tuberculosis, available online at https://doi.org/10.1016/j.tube.2021.102088. It is not the copy of record. Copyright © 2021, Elsevier.

FUNDING.

This research did not receive any specific grant from funding agencies in the public, commercial, or not-for-profit sectors.

DECLARATIONS OF INTEREST: none.

This is an accepted manuscript of an article published by Elsevier in Tuberculosis, available online at https://doi.org/10.1016/j.tube.2021.102088. It is not the copy of record. Copyright © 2021, Elsevier.

403 **REFERENCES.**

404

405 [1]. Dawson H, Robson Brown K. Childhood tuberculosis: A Probable Case from Late Mediaeval
406 Somerset, England. 2012; Int J Osteoarchaeol **2:** 31 35. https://doi.org/10.1016/j.ijpp.2012.04.001

407

408 [2]. Gathercole C. An Archaeological Assessment of Taunton (English Heritage Extensive Urban
409 Survey), 2002; (Taunton), **7**.

410

411 [3]. Dawson H, Unearthing Late Medieval Children: Health status and burial practice in Southern
412 England. British Archaeological Reports British Series 593. Oxford: Archaeopress; 2014.

413

414 [4]. Santos AL, Roberts CA. A picture of tuberculosis in young Portuguese people in the early 20th
415 century: a multidisciplinary study of the skeletal and historical evidence. 2001; Am J Phys
416 Anthropol **115:** 38–49. https://doi.org/10.1002/ajpa.1054

417

418 [5]. Angelini A, Mavrogenis AF, Rimondi E, Rossi G, Ruggieri P. Current concepts for the diagnosis
419 and management of eosinophilic granuloma of bone. 2017; J Orthop Traumatol **18:** 83-90.
420 https://doi.org/10.1007/s10195-016-0434-7

421

422 [6]. Schour I, Massler M. The development of the human dentition. 1941; J Am Dent Assoc **28**:
423 1153-1160.

424

425 [7]. Taylor GM, Murphy EM, Mendum TA, Pike AWG, Linscott B, Wu H, O'Grady J, Richardson H,
426 O'Donovan E, Troy C, Stewart G. Leprosy at the Edge of Europe – Biomolecular, Isotopic and
427 Osteoarchaeological Findings from Medieval Ireland. 2018; PLoS One **13:** e0209495.
428 https://doi.org/10.1371/journal.pone.0209495.

429

430 [8]. Boom R, Sol CJ, Salimans MM, Jansen CL, Wertheim-van Dillen PM, van der Noordaa J. Rapid
431 and simple method for purification of nucleic acids. 1990; J Clin Microbiol **28:** 495–503. PMID:
432 1691208

433

This is an accepted manuscript of an article published by Elsevier in Tuberculosis, available online at https://doi.org/10.1016/j.tube.2021.102088. It is not the copy of record. Copyright © 2021, Elsevier.

[9]. Taylor GM, Crossey M, Saldanha JA, Waldron T. Detection of *Mycobacterium tuberculosis* bacterial DNA in medieval human skeletal remains using polymerase chain reaction. 1996; J Archaeol Sci **23:** 789-798. https://doi.org/10.1006/jasc.1996.0073.

[10]. Thierry D, Cave MD, Eisenach KD, Crawford JT, Bates J, Gicquel B, Guesdon JL. IS-*6110*, an IS-like element of *Mycobacterium tuberculosis* complex. 1990; Nucleic Acids Research **18:** 188. https://doi.org/10.1093/nar/18.1.188.

[11]. Roychowdhury S, Mandal S, Bhattacharya A. Analysis of IS*6110* insertion sites provide a glimpse Into genome evolution of *Mycobacterium tuberculosis*. 2015; Sci Rep **28:** 12567. https://doi.org/10.1038/srep12567.

[12]. Huyen MN, Tiemersma EW, Kremer K, de Haas P, Lan NT, Buu TN, Sola C, Cobelens FG, van Soolingen D. Characterisation of *Mycobacterium tuberculosis* isolates lacking IS6110 in Viet Nam. 2013; Int J Tuberc Lung Dis. **17**: 1479-1485. https://doi.org/10.5588/ijtld.13.0149.

[13]. Taylor GM, Stewart GR, Cooke M, Chaplin S, Ladva, S, Kirkup J, Palmer S and Young DB. Koch's Bacillus – A Look at the First Isolate of M. *tuberculosis* from a Modern Perspective. 2003; Microbiology **149:** 3213-3220. https://doi.org/10.1099/mic.0.26654-0.

[14]. Mays S, Ogden A, Montgomery J, Vincent S, Battersby W, Taylor GM. New light on the personal identification of a skeleton of a crew member of Sir John Franklin's last expedition to the arctic, 1845. 2011; J Archaeol Sci **38:** 1571-1582. https://doi.org/10.1016/j.jas.2011.02.022.

[15]. Liébana, Aranaz A, Francis B, Cousins D. Assessment of genetic markers for species differentiation within the *Mycobacteria tuberculosis* complex. 1996; J Clin Microbiol **34:** 933–938. https://doi.org/10.1128/JCM.34.4.933-938.1996.

[16]. Weil A, Pliyatis BB, Butler WR, Woodley CL, Shinnick TM. The *mtp40* gene is not present in all strains of *Mycobacterium tuberculosis*. 1996; J Clin Microbiol **34**: 2309–2311. https://doi.org/10.1128/jcm.34.9.2309-2311.1996.

This is an accepted manuscript of an article published by Elsevier in Tuberculosis, available online at https://doi.org/10.1016/j.tube.2021.102088. It is not the copy of record. Copyright © 2021, Elsevier.

466 [17]. Koivula T, Svenson SB, Kallenius, G. The *mtp40* gene is not present in *Mycobacterium bovis.*
467 *2002;* Tuberculosis (Edinb) **82**: 183-185. https://doi.org/10.1054/tube.2002.0338.
468
469 [18]. Gordon SV, Brosch R, Billaut A, Garnier T, Eiglemeier K, Cole ST. Identification of variable
470 regions in the genomes of tubercle bacilli using bacterial artificial chromosome arrays. 1999; Mol
471 Microbiol **32:** 643–655. https://doi.org/10.1046/j.1365-2958.1999.01383.x
472
473 [19]. Constant P, Perez E, Malaga W, Lanéelle MA, Saurel O, Daffé M, Guilhot C. Role of the
474 pks15/1 gene in the biosynthesis of phenolglycolipids in the Mycobacterium tuberculosis complex.
475 Evidence that all strains synthesize glycosylated p-hydroxybenzoic methyl esters and that strains
476 devoid of phenolglycolipids harbor a frameshift mutation in the pks15/1 gene. 2002; J Biol Chem
477 **277**(41): 38148-38158. https://doi: 10.1074/jbc.M206538200.
478
479 [20]. Ortner DJ. Identification of Pathological Conditions in Human Skeletal Remains. London:
480 Academic Press; 2003.
481
482 [21]. Bendrey R, Cassidy J, Fournié G, Merrett D, Oakes R, Taylor, GM. Approaching ancient disease
483 from a One Health perspective: interdisciplinary review for the investigation of zoonotic
484 brucellosis. 2020; Int J Osteoarchaeol **30:** 99-108. https://doi.org/10.1002/oa.2837.
485
486 [22]. Waldron HA, Taylor GM, Rudling DR. Sexing of Romano-British Baby Burials From the
487 Beddingham Roman Villa, East Sussex. 1999; Sussex Archaeological Collections **137**: 71-79.
488 https://doi.org/10.5284/1000334.
489
490 [23]. Sidstedt M, Jansson L, Nilsson E, Forsman M, Rådström P, Hedman J. Humic substances cause
491 fluorescence inhibition in real-time polymerase chain reaction. 2015; Anal Biochem **487:** 30-37.
492 https://doi.org/10.1016/j.ab.2015.07.002.
493
494 [24]. Matheson C, Gurney C, Esau N, Lehto R. Assessing PCR Inhibition from humic substances.
495 2010; Open Enzym Inhib J **3:** 38-45. https://doi.org/ 10.2174/1874940201003010038.
496
497 [25]. Gagneux S, DeReimer K, Van T, Kato-Maeda M, et al. Variable host–pathogen compatibility in
498 *Mycobacterium tuberculosis*. 2006; Proc Natl Acad Sci USA **103:** 2869–2873.

This is an accepted manuscript of an article published by Elsevier in Tuberculosis, available online at https://doi.org/10.1016/j.tube.2021.102088. It is not the copy of record. Copyright © 2021, Elsevier.

https://doi.org/10.1073/pnas.0511240103.

[26]. Badalian-Very G, Vergilio JA, Degar BA, MacConaill LE, Brandner B, Calicchio ML, Kuo FC, Ligon AH, Stevenson KE, Kehoe SM, Garraway LA, Hahn WC, Meyerson M, Fleming MD, Rollins BJ. Recurrent BRAF mutations in Langerhans cell histiocytosis. 2010; Blood **116**(11): 1919-1923. https://doi: 10.1182/blood-2010-04-279083.

[27]. Hertz D, Schneider B. Sex differences in tuberculosis. 2019; Semin Immunopathol **41:** 225-237. https://doi.org/10.1007/s00281-018-0725-6.

[28]. Rao S. Tuberculosis and patient gender. An analysis and its implications in tuberculosis control. 2009; Lung India **26:** 46-47. https://doi.org.10.4103/0970-2113.48897.

[29]. Resnick D, Niwayama G. Osteomyelitis, septic arthritis, and soft tissue infection: Organisms. 1995; in: Resnick D, editor. Diagnosis of bone and joint disorders. Edinburgh: Saunders. P 2448–2558.

[30]. Lamb GS, Starke JR. Tuberculosis in infants and children. 2017; Microbiol Spectr **5**(2): TNMI7-0037-2016. https://doi.org/10.1128/9781555819866.ch32.

[31]. Wallgren A. (1948). The time-table of tuberculosis. Tubercle **29**(11): 245-51. Https://doi: 10.1016/s0041-3879 (48) 80033-4.

[32]. Maltezou HC, Spyridis P, Kafetzis DA. Extra-pulmonary tuberculosis in children. 2000; Arch. Dis. Child. **83:** 342-346. https:// doi: 10.1136/adc.83.4.342.

[33]. Raut AA, Nagar AM, Muzumdar D, Chawla AJ, Narlawar RS, Fattepurka S, Bhatgadde VL. 2004 Imaging features of calvarial tuberculosis: A study of 42 cases. 2004; Am J Neuroradiol **25:** 409-414. PMID: 15037463.

[34]. Datta SGS, Bhatnagar V, Pan S, Mehta R, Sharma C. Primary calvaria tuberculosis: a report of three cases. 2019; Brit J Neurosurg **33**(2): 196-201. https://doi: 10.1080/02688697.2017.1409879.

This is an accepted manuscript of an article published by Elsevier in Tuberculosis, available online at https://doi.org/10.1016/j.tube.2021.102088. It is not the copy of record. Copyright © 2021, Elsevier.

[35]. Columbo A, Saint-Pierre C, Naji S, Panuel M, Coqueugniot H, Dutour O. Langerhans cell histiocytosis or tuberculosis on a medieval child (Oppidum de al Granede, Millau, France – 10th-11th centuries AD). 2015; Tuberculosis **95**: S42-S50. https://doi: 10.1016/j.tube.2015.02.003.

[36]. Abegg C, Dutour O, Desideri J, Besse M. Cases of *serpens endocrania symmetrica* in young individuals from Neolithic Western Switzerland: Description and interpretation. 2020; Int J Osteoarchaeol **30**: 401–409. https://doi.org/10.1002/oa.2863.

[37]. Geber J. Victims of Ireland's great famine: The bioarchaeology of mass burials at Kilkenny Union Workhouse. Florida: University Press of Florida; 2015.

[38]. Hershkovitz I, Donoghue H D, Minnikin D E, May H, Lee O Y-C, Feldman M, Galili E, Spigelman M, Rothschild B M, Bar-Gal G K. Tuberculosis origin: The Neolithic scenario. 2015; Tuberculosis **95:** S122-S126. https://doi: 10.1016/j.tube.2015.02.021.

[39]. Collins C. Tuberculosis in medieval Iceland: evidence from Hofstaðir, Keldudalur and Skeljastaðir. 2020; Homo **71**(4): 299-316. https://doi: 10.1127/homo/2020/1098.

[40]. Hlavenková L, Teasdale M D, Gábor O, Nagy G, Beňuš R, Marcsik A, Pinhasi R, Hajdu T. Childhood bone tuberculosis from Roman Pécs, Hungary. 2015; Homo **66**(1): 27-37. https://doi: 10.1016/j.jchb.2014.10.001

[41]. Lewis M. Palaeopathology of Children: Identification of pathological conditions in the human skeletal remains of non-adults. London: Academic Press; 2018.

[42]. Spekker O, Kis L, Deák A, Makai E, Pálfi G, Váradi OA, Molnár E. An unusual case of childhood osteoarticular tuberculosis from the Árpádian Age cemetery of Győrszentiván-Revhegyi tag (Győr-Moson-Sopron county, Hungary). 2021; PLoS ONE **16**(4): e0249939. https://doi.org/10.1371/journal.pone.0249939.

[43]. Sparacello VS, Roberts CA, Kerudinc A, Müller, R. A 6500-year-old Middle Neolithic child from Pollera Cave (Liguria, Italy) with probable multifocal osteoarticular tuberculosis. 2017; Int J Paleopathol **17**: 67–74. https://doi.org/10.1016/j.ijpp.2017.01.004

This is an accepted manuscript of an article published by Elsevier in Tuberculosis, available online at https://doi.org/10.1016/j.tube.2021.102088. It is not the copy of record. Copyright © 2021, Elsevier.

564 [44]. Walker D. Disease in London, 1st -19th centuries: An illustrated guide to diagnosis, MOLA
565 monograph 56. London: Museum of London Archaeology; 2012.
566
567 [45]. Palfi G, Bereczki Z, Ortner D J, Dutour O. Juvenile cases of skeletal tuberculosis from the Terry
568 anatomical collection (Smithsonian Institution, Washington, D. C., USA). 2012; Acta Biologica
569 Szegediensis **56**(1): 1-12. https://doi: 10.1016/j.jchb.2014.10.001.
570
571 [46]. Taylor GM, Young DB, Mays SA. Genotypic Analysis of the Earliest Known Prehistoric Case of
572 Tuberculosis from Britain. 2005; J Clin Microbiol **43:** 2236-2240.
573 https://doi.org/10.1128/JCM.43.5.2236-2240.2005.
574
575 [47]. Müller R, Roberts CA, Brown TA. Biomolecular Identification of Ancient *Mycobacterium*
576 *tuberculosis* Complex DNA in Human Remains From Britain and Continental Europe. 2014; Am J
577 Phys Anthropol **153:** 178–189. https://doi.org/10.1002/ajpa.22417.
578
579 [48]. Mays SA, Taylor GM, Legge AJ, Young DB, Turner-Walker G. A Palaepathological and
580 biomolecular study of tuberculosis in a medieval skeletal collection from England. 2001; Am J Phys
581 Anthropol **114:** 298-311. https://doi.org/10.1002/ajpa.1042.
582
583 [49]. Kamerbeek J, Schouls L, Kolk A, van Agterveld M, van Soolingen D, Kuijper S, Bunshoten A,
584 Molhuizen H, Shaw R, Goyal M, van Embden J. Simultaneous detection and strain differentiation of
585 *Mycobacterium tuberculosis* for diagnosis and epidemiology. 1997; J Clin Microbiol **35:** 907–914.
586 https://doi.org/10.1128/JCM.35.4.907-914.1997.
587
588 [50]. Mays S, Fysh E, Taylor GM. Periostitic rib lesions – a sign of pulmonary tuberculosis? 2002;
589 Am J Phys Anthropol **119:** 27-36. https://doi.org/10.1002/ajpa.10099.
590
591 [51]. Mays S, Taylor GM. Osteological and biomolecular study of two possible cases of
592 hypertrophic osteoarthropathy from Mediaeval England. 2002; J Archaeol Sci 29**:** 1267-1276.
593 https://doi.org/10.1006/jasc.2001.0769.
594
595 [52]. Bouwman AS, Kennedy SL, Müller R, Stephens RH, Holst M, Caffell AC, Roberts CA, Brown TA.
596 Genotype of a historic strain of *Mycobacterium tuberculosis*. 2012; Proc Natl Acad Sci USA **109:**

This is an accepted manuscript of an article published by Elsevier in Tuberculosis, available online at https://doi.org/10.1016/j.tube.2021.102088. It is not the copy of record. Copyright © 2021, Elsevier.

597 18511-18516. https://doi.org/10.1073/pnas.120944410.
598

This is an accepted manuscript of an article published by Elsevier in Tuberculosis, available online at https://doi.org/10.1016/j.tube.2021.102088. It is not the copy of record. Copyright © 2021, Elsevier.

599 **TABLES.**

600

601 **Table 1.**

IS1081 PCR	Amplicon size (bp)	Result	
		Expt.1	Expt.2
Primers F2/R2	135	- (no Cq)	- (no Cq)
Primers F2/R3	113	- (no Cq)	- (no Cq)
Primers F3/R3	79	+ (38.2)	+ (36.7)

602

603 Table 1 caption.

604 Sk2077 atlas extract screened for MTB complex using the IS*1081* PCR with product reported using

605 a specific HEX-BHQ1 dual-labelled hybridization probe with various primer combinations.

606 + = PCR positive and – = PCR negative. Cycle threshold values (Cq, mean of duplicates) are given

607 below positive results.

608

This is an accepted manuscript of an article published by Elsevier in Tuberculosis, available online at https://doi.org/10.1016/j.tube.2021.102088. It is not the copy of record. Copyright © 2021, Elsevier.

609 **Table 2.**

Location	Period	Age	Description	Reference
Atlit-Yam	Neo	0-1 year	Endocranial lesions and periosteal new bone formation on long bones, aDNA confirmation	Hershkovitz et al. (2015) [38]
Italy	Neo	5 yrs	Pitting and cavitation on the inferior surface of the body of the fourth cervical vertebra alongside evidence for lytic lesions on the ribs and some PNB on the long bones	Sparacello et al. (2017) [43]
Sion Chemin des Collines, Switzerland	Neo	8 ±2 yrs	Endocranial lesions (SES), periostitis on the tibia	Abegg et al. (2020) [36]
		1-2 yrs	Endocranial lesions (SES)	
Sion Petit-Chasseur, Switzerland	Neo	4 ±2 yrs	Small circular lesion on the right parietal, SES on occipital	
Pécs, Hungary	Roman	9-10	Lytic lesions on ribs and vertebrae, PNB on long bones	Hlavenková et al. (2015) [40]
France	Med	1-2.5 yrs	lytic lesions on the cranium	Columbo et al. (2015) [35]
Hofstaðir, Iceland	Med	2-5 mo	lytic lesions and plaque-like bone on the atlas and some vertebral arches	Collins (2020) [39]
Skeljastaðir, Iceland	Med	12-14 yrs	Endocranial lesions of the occipital, visceral surface lesions of multiple ribs, destructive lesions of vertebral bodies C5-7, periosteal reaction on dorsal atlas	
Győrszentiván-Revhegyi tag, Hungary	Med	12 yrs	Destructive lesions of the vertebrae including pitting on C1-C5 and rib ends	Spekker et al. (2021) [42]
Kilkenny Union Workhouse, Ireland	PM	9 yrs	Osteolytic crater on the frontal bone	Geber (2015) [37]
Terry anatomical collection	PM	17 yrs	Destructive lesions of the vertebrae including the atlas	Palfi et al. (2012) [45]
Bow Baptist church, London	PM	7 yrs	Destruction of vertebral bodies including C5-7, pitting on visceral surface of the ribs	Walker (2012) [44]
St Marylebone old	PM	2 yrs	Lytic lesions of cervical spine	

This is an accepted manuscript of an article published by Elsevier in Tuberculosis, available online at https://doi.org/10.1016/j.tube.2021.102088. It is not the copy of record. Copyright © 2021, Elsevier.

church			
St Mary & St Michael	PM	1 year	C5-7 lytic activity and remodelling on the laminae

610

611 Table 2 caption.

612 Comparative archaeological cases of child tuberculosis published since 2012.

613 Neo = Neolithic; Med = Mediaeval; PM = Post Mediaeval. PNB = periosteal new bone.

614

This is an accepted manuscript of an article published by Elsevier in Tuberculosis, available online at https://doi.org/10.1016/j.tube.2021.102088. It is not the copy of record. Copyright © 2021, Elsevier.

CAPTIONS TO FIGURES.

Figure 1a. Plan of the excavation areas of the Taunton priory cemetery which took place in 2005. The location of the remains of Sk2077 in area 4 are shown by the red dot.

Figure 1b. The East-facing burial of Sk2077 photographed during excavation of the site. *Post mortem* damage is seen on the cranium on the left parietal bone.

Figure 2. Real time PCR for the IS*6110* element of MTB complex applied to Sk2077 extracts prepared from a rib and the cervical vertebra. Panel a): Amplification profiles from rib 1 without lesion (blue traces) and the cervical vertebra (pink traces). Panel b): Dissociation analyses from the same experiment with specific product showing a melt temperature of around 90.5C. Experiments were run on an MxPro 3005P real-time platform (Agilent Technologies).

Figure 3. IS*1081* real-time PCR amplification profiles for Sk2077 atlas (red traces) and for two template blanks (black traces). IS*1081* product amplified using primer pair F3/R3 was reported with a HEX labelled specific hybridization probe. These are the results of experiment 2 mentioned in Table 1.

Figure 4. Gel electrophoretic separation of IS*6110* and *mtp40* PCR products from Sk2077 run on 3% agarose. Lanes 1 and 2 = IS*6110* PCR product (123-bp). Lanes 3 and 4 = template blanks. Lane L = 100-bp DNA size markers. Bright band (arrowed) represents 500-bp size marker. Lanes 5 and 6: *mtp40* PCR product (113-bp). Lanes 7 and 8: Template blanks for the *mtp40* PCR experiment.

Figure 5. Upper panel a): Real-time PCR amplification profile of the pks15/1 locus from Sk2077 (blue traces) and a water blank (black trace) with product monitored with a specific dual-labelled hydrolysis probe. Lower panel b) shows sequencing of the purified PCR product with position of the 7-bp deletion (GGGCCGC) [19] highlighted in yellow.

Figure 6, panel a). Dissociation (melt) curve analyses of amelogenin PCR showing profiles of male subject DNA (blue trace, two peaks), female subject DNA (red trace, one peak) and rib extract from Sk2077 (green trace, one peak). A template or water blank negative control is included (black trace, flatline). Note same Tmelt of Sk2077 as the smaller male peak from reference male DNA at 79.7C.

This is an accepted manuscript of an article published by Elsevier in Tuberculosis, available online at https://doi.org/10.1016/j.tube.2021.102088. It is not the copy of record. Copyright © 2021, Elsevier.

Figure 6, panel b). Extended gel electrophoretic separation of products from the same experiment shown in panel a). Lane 1 = template blank. Lane 2 = Sk2077 rib product. Lanes 3 and 4, nil. Lanes 5 and 6 contain male and female reference DNA respectively. Lane 7 shows 100-bp DNA size markers for comparison. Position of arrow indicates position of expected 105-bp Y chromosome product generated from Sk2077.

This is an accepted manuscript of an article published by Elsevier in Tuberculosis, available online at https://doi.org/10.1016/j.tube.2021.102088. It is not the copy of record. Copyright © 2021, Elsevier.

FIGURES.

Figure 1.

a).

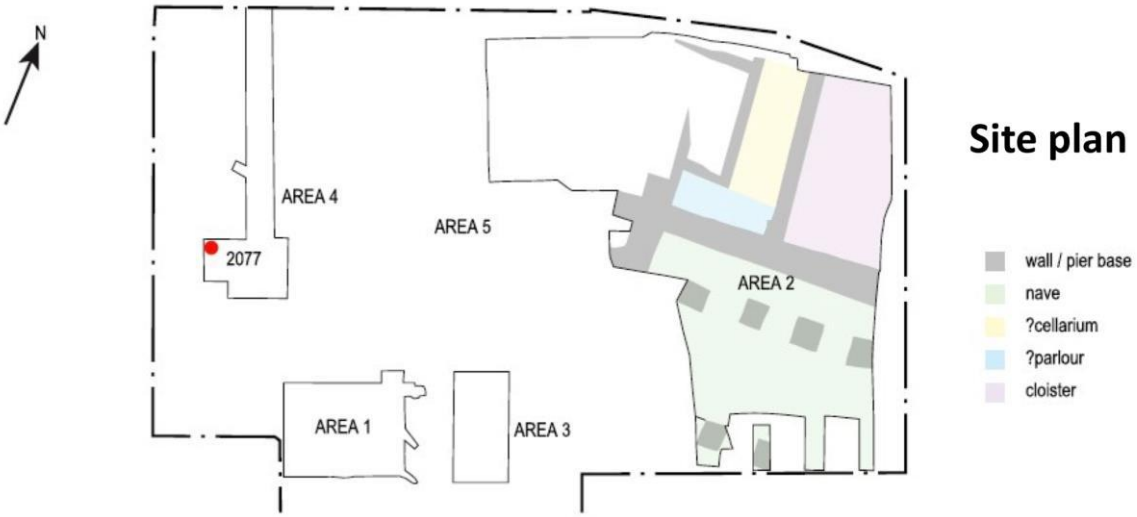

b).

This is an accepted manuscript of an article published by Elsevier in Tuberculosis, available online at https://doi.org/10.1016/j.tube.2021.102088. It is not the copy of record. Copyright © 2021, Elsevier.

659 Figure 2.

660

a).

b).

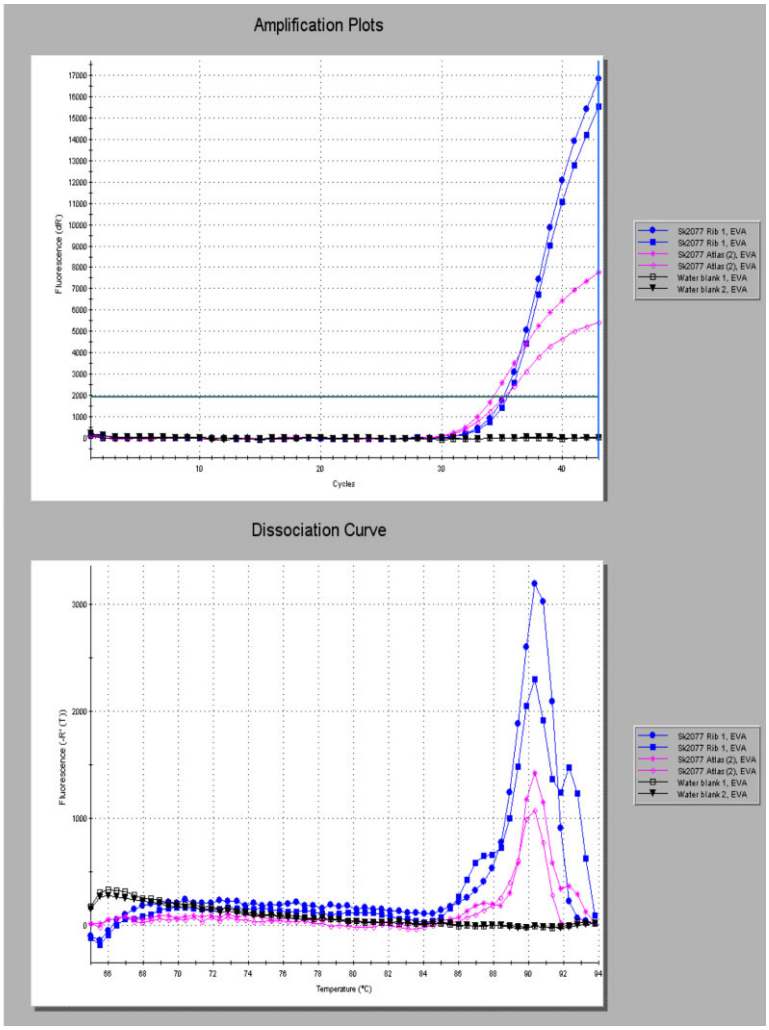

661

662

663

664 Figure 3.

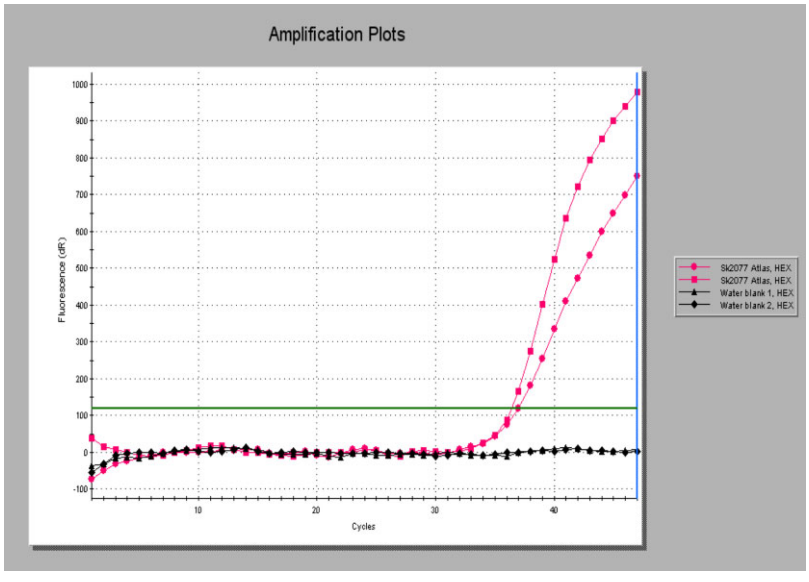

665

This is an accepted manuscript of an article published by Elsevier in Tuberculosis, available online at https://doi.org/10.1016/j.tube.2021.102088. It is not the copy of record. Copyright © 2021, Elsevier.

Figure 4.

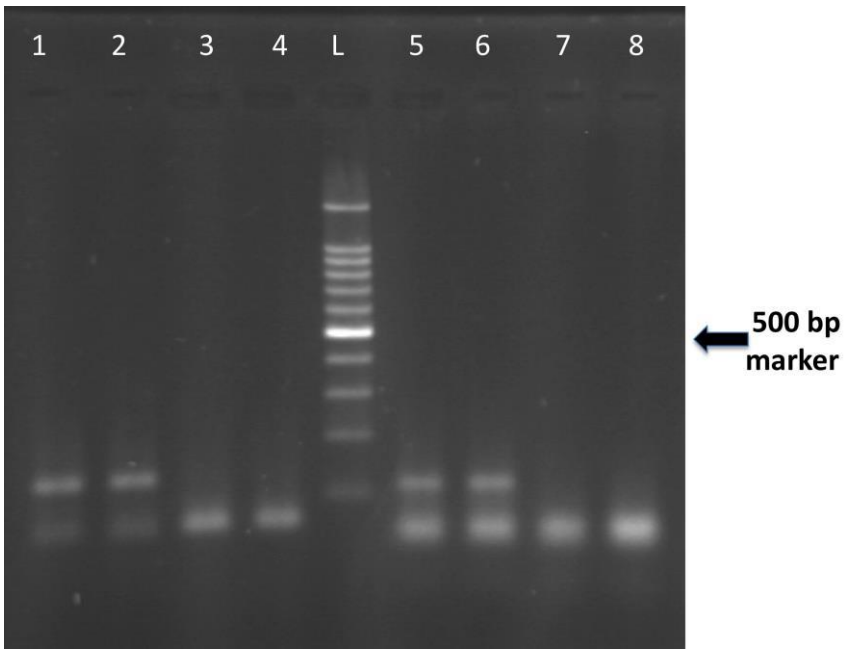

Figure 5.

a).

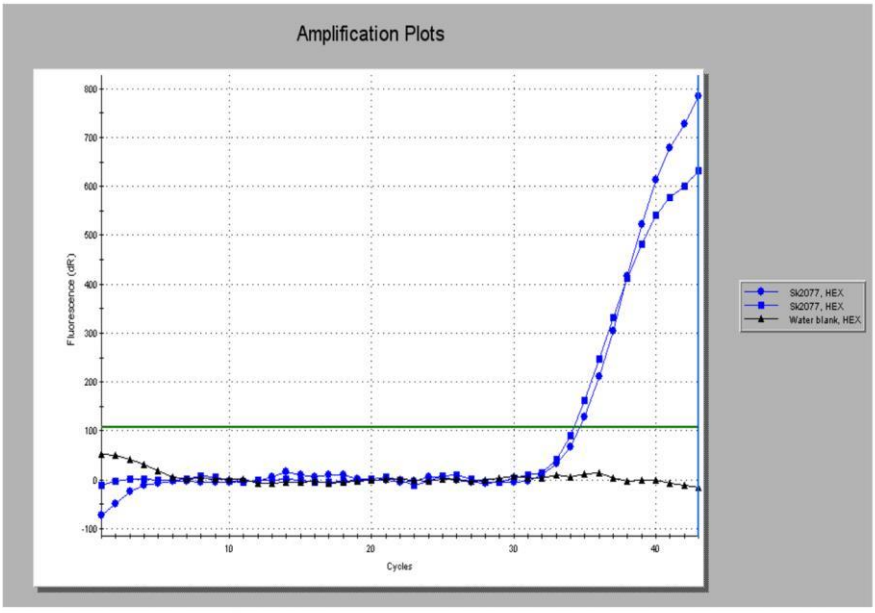

b).

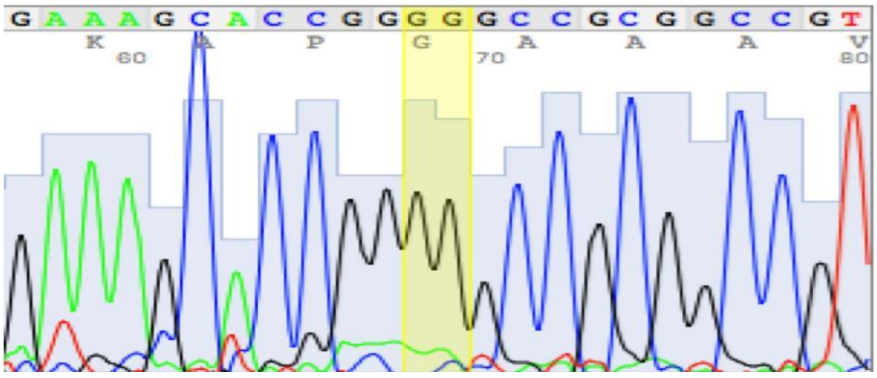

This is an accepted manuscript of an article published by Elsevier in Tuberculosis, available online at https://doi.org/10.1016/j.tube.2021.102088. It is not the copy of record. Copyright © 2021, Elsevier.

673 Figure 6.

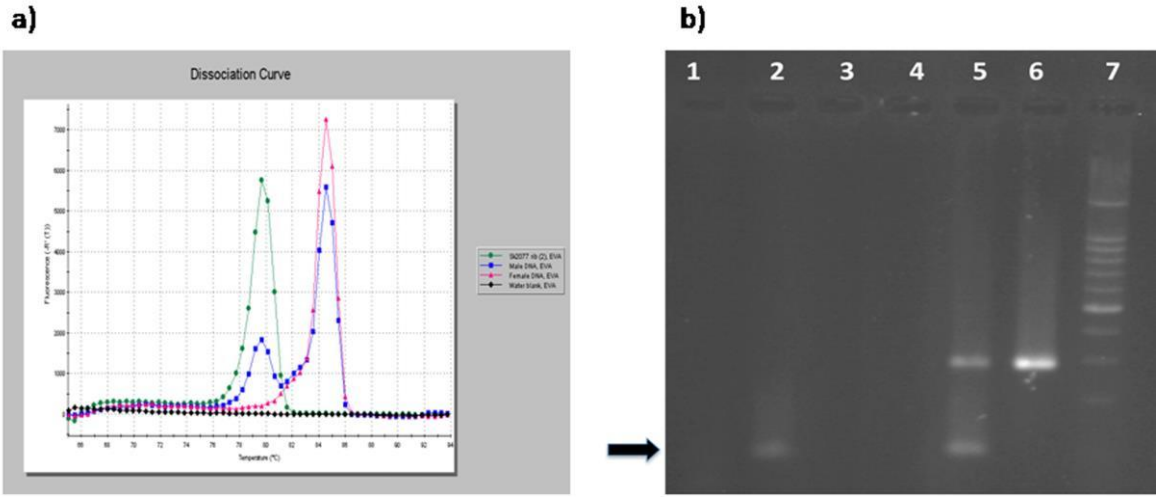

674

675

This is an accepted manuscript of an article published by Elsevier in Tuberculosis, available online at https://doi.org/10.1016/j.tube.2021.102088. It is not the copy of record. Copyright © 2021, Elsevier.